Chapter 2

Structural Foundations for O_2 Sensitivity and O_2 Tolerance in [NiFe]-Hydrogenases

Anne Volbeda and Juan C. Fontecilla-Camps*
Metalloproteins Unit, Institut de Biologie Structurale J.P. Ebel, Commissariat à l'Énergie Atomique, Centre National de la Recherche Scientifique, Université Joseph Fourier, UMR 5075, 41 rue Jules Horowitz, 38027 Grenoble, France

Summary

Nature has evolved three different ways of metabolizing hydrogen, represented by the anaerobic [Fe]-, [FeFe]- and [NiFe]-hydrogenases. Structural and functional studies of these enzymes have unveiled the unusual composition of their active sites and characterized their catalytic mechanisms. From a biotechnological viewpoint, the most interesting hydrogenases are those that contain a [NiFe] moiety in their active sites. Some of these enzymes are O_2-resistant and can rapidly reductively recover from oxygen exposure whereas others are O_2-tolerant and can oxidize H_2 even at atmospheric oxygen levels. O_2-resistant [NiFeSe]-hydrogenases have one of the Cys ligands of the active site replaced by a SeCys and do not display the hard-to-reactivate "unready" state provoked by O_2. The reasons for this property might be related to the formation of O_2-derived Se-O bonds, which are weaker than

*Author for correspondence, e-mail: juan.fontecilla@ibs.fr

D. Zannoni and R. De Philippis (eds.), Microbial BioEnergy: Hydrogen Production, Advances in Photosynthesis and Respiration 38, pp. 23–41, DOI 10.1007/978-94-017-8554-9_2,

S-O bonds and, consequently, easier to break upon reduction. Conversely, membrane-bound O_2-tolerant hydrogenases have an unusual proximal (relative to the active site) [Fe_4S_3] cluster coordinated by six Cys ligands. This cluster can rapidly send two successive electrons to the active site helping to reduce oxygen to water there. Some microorganisms posses more than one hydrogenase and use them in different ways. For instance, there are three well-characterized [NiFe]-hydrogenases in the model bacterium *Escherichia coli*. They are highly regulated and each one plays a specific role: microaerobic/anaerobic H_2 uptake, anaerobic H_2 evolution and, protection from O_2-induced damage, respectively. These enzymes are discussed in connection with the metabolic changes *E. coli* undergoes during its transit through the intestinal tract of the host. O_2-tolerant hydrogenases have been used to build bio-fuel cells that can function under air. Also, O_2-resistant [NiFeSe]-hydrogenases have been attached to TiO_2 particules for H_2 production from solar energy. Hydrogenase active sites have also served as a source of inspiration for the synthesis of organometallic catalysts.

I. Introduction

Many microorganisms use enzymes called hydrogenases to oxidize molecular hydrogen or reduce protons according to the reaction $H_2 \leftrightarrow 2H^+ + 2e^-$. Two major unrelated enzyme classes exist: the [FeFe]- and the [NiFe]-hydrogenases (Vignais and Billoud 2007; Fontecilla-Camps et al. 2007). The former are found in bacteria and some green algae, fungi and protozoa, whereas the latter are widespread in both bacteria and archaeans but absent from eukaryotes. A special class of enzymes called [Fe]-hydrogenases couples H_2 oxidation with the reduction of methenyl-tetrahydromethanopterin (HC-H_4MPT$^+$) without electron transfer to an external redox partner. When provided with the reaction products, H^+ + H_2C-H^{4}MPT, H_2 is evolved (Thauer et al. 2010). In general, [Fe]-hydrogenases, which are only found in archaeal species, are irreversibly inactivated by O_2. [FeFe]-hydrogenases are generally more active in proton reduction than [NiFe]- hydrogenases, which are more biased to H_2 oxidation. However, there are exceptions to this rule, such as the periplasmic [FeFe]-hydrogenase from *Desulfovibrio desulfuricans* which is an uptake enzyme (Nicolet et al. 1999). Proton reduction is physiologically important to eliminate excessive reducing power generated by photosynthetic and fermentative processes. Conversely, microorganisms can use the low-potential electrons generated by hydrogen oxidation for respiration with different terminal electron acceptors such as, for example, fumarate, nitrate, carbon dioxide, sulfur, sulfate, the heterodisulfide CoM-S-S-CoB (between coenzyme M and coenzyme B) in methanogenic archaeans and, in some exceptional cases, dioxygen. Hydrogen oxidation is also used to recycle H_2 generated by nitrogenases during N_2 reduction to ammonia by azototrophic bacteria.

[FeFe]-hydrogenases are generally O_2-sensitive but can be reactivated if they are progressively exposed to this gas, like is the case during aerobic purification. However, in the presence of excessive reducing power the enzyme metal centers can be irreversibly damaged due to the formation of radical oxygen species. In general, such sensitivity towards O_2 is a stumbling block for biotechnological applications. Conversely, many [NiFe]-hydrogenases are, at least in vitro, only reversibly inactivated by O_2 and some are present in aerobic organisms that can couple hydrogen oxidation to oxygen reduction. Because of these interesting properties we will now discuss this class of enzymes in more detail.

Abbreviations: EPR – Electron Paramagnetic Resonance spectroscopy; FTIR – Fourier Transform InfraRed spectroscopy; Pt – Platinum; TiO_2 – Titanium dioxide

II. [NiFe]-Hydrogenases

A. Types of [NiFe]-Hydrogenases

The simplest [NiFe]-hydrogenase consists of a large subunit containing the active Ni-Fe site and a small subunit typically harboring a proximal [Fe_4S_4], a medial [Fe_3S_4] and a distal [Fe_4S_4] cluster, which transfer electrons to and from the active site, located in the large subunit (Fig. 2.1a). Exceptions are the [NiFeSe]-hydrogenases that have a medial [Fe_4S_4] cluster and the O_2-tolerant enzymes that contain a modified proximal [Fe_4S_3] cluster (see below). [NiFe]-hydrogenases are either periplasmic or cytoplasmic H_2-uptake enzymes. Heterodimeric cytoplasmic enzymes typically function in the recycling of H_2 produced by microbial nitrogenases, as in cyanobacteria (Bothe et al. 2010, see also Chaps. 6 and 8). Heterodimeric periplasmic [NiFe]-hydrogenases have been extensively studied in sulfate-reducing bacteria (Fontecilla-Camps et al. 2007). They allow these organisms to use H_2 as an electron donor for the reduction of sulfate via a complex and still incompletely characterized electron transfer pathway, reviewed by Matias et al. (2005), that starts with a water-soluble cytochrome c_3 electron carrier. Based on sequence homologies (Vignais and Billoud 2007), all [NiFe]-hydrogenases have a common heterodimeric core that resembles the first structure of the enzyme from *Desulfivibrio gigas* published by Volbeda et al. (1995). In most hydrogenases this basic core forms part of larger protein complexes with different redox partners, including quinones in the cytoplasmic membrane and ferredoxin, NAD or NADP in the cytoplasm. In methanogenic archaea the quinones are replaced by methanophenazine and NAD is normally replaced by coenzyme F_{420} (8-hydroxy-5-deazaflavin), although there are also hyperthermophilic archaea that use NADP (Horch et al. 2012). In addition, methanogens have hydrogenases that are coupled with a heterodisulfide reductase to reduce the S-S bond between coenzymes M and B, produced in the last step of methanogenesis (Thauer et al. 2010).

Many of the multi-subunit complexes show striking homologies with NADH: ubiquinone oxidoreductase, also known as respiratory complex I. Although the latter does not have a Ni-Fe active site, the homology extends even to the basic heterodimeric hydrogenase core. The known structure and organization of both the hydrophilic and membrane-bound hydrophobic subunits of complex I has been used to construct homology-based models of several multisubunit hydrogenases (Efremov and Sazanov 2012). These include the so-called bidirectional hydrogenases, reviewed by Horch et al. (2012),

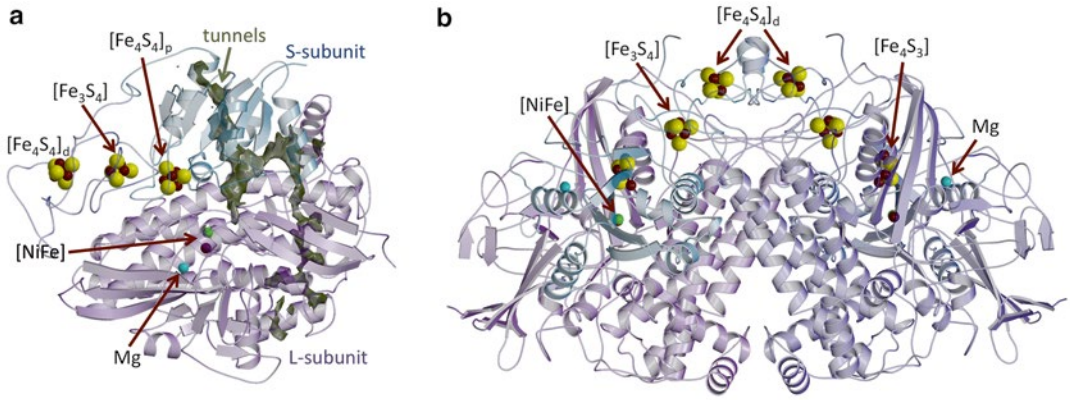

Fig. 2.1. Basic structural organization of [NiFe]-hydrogenases: (**a**) the heterodimeric (SL) oxygen-sensitive enzyme of *Desulfovibrio fructosovorans*; (**b**) the heterotetrameric $(SL)_2$ oxygen-tolerant hydrogenase-1 of *Escherichia coli.*

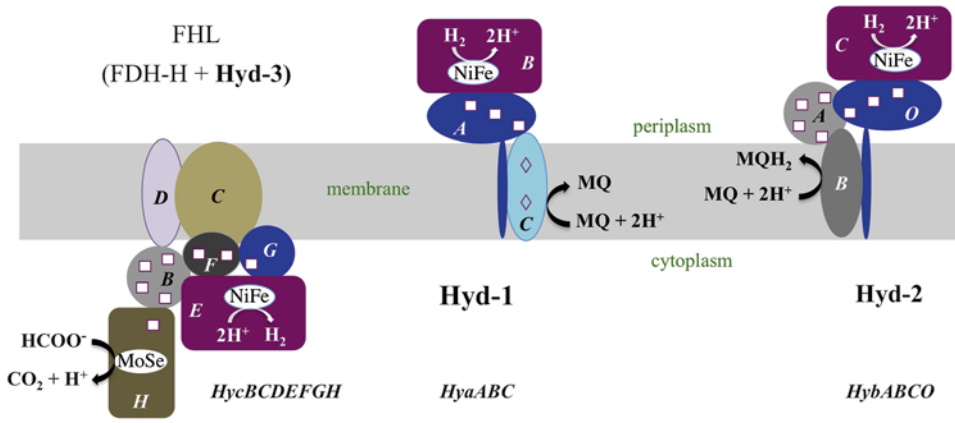

Fig. 2.2. Multisubunit complexes of the three *E. coli* [NiFe]-hydrogenases *Ec*Hyd-1, *Ec*Hyd-2 and *Ec*Hyd-3. The latter is part of the formate:hydrogenase lyase (FHL) complex which contains also formate dehydrogenase H (FDH-H). Electron-transferring iron-sulfur clusters are highlighted as squares, *b*-type hemes as diamonds and active sites as ellipsoids. MQ and MQH_2 are the oxidized and reduced forms of menaquinone. Subunits are labeled with capital letters, the corresponding genes are given in *italics* underneath.

which are found, for example, in the cytoplasm of photosynthetic bacteria. These enzymes typically consist of five different subunits in Bacteria and three in Archaea, and exchange electrons with either NAD(P) or coenzyme F_{420}, via a flavin-containing diaphorase subunit. The O_2-tolerant soluble [NiFe]-hydrogenase of *Ralstonia eutropha* (*Re*MBH) is also a member of this group of enzymes. Other multisubunit hydrogenases related to complex I are the proton pumping energy converting hydrogenases (Ech) found in the membrane fraction of Archaea like *Methanosarcina barkeri*, which use a ferredoxin as redox partner and consist of at least six subunits (Hedderich 2004), and *Ec*Hyd-3, which is a H_2 evolving hydrogenase of the enteric bacterium the *Escherichia coli*.

B. The [NiFe]-Hydrogenases of Escherichia coli

This enteric anaerobic bacterium has three well-studied multisubunit [NiFe]-hydrogenases (Fig. 2.2) called *Ec*Hyd-1, *Ec*Hyd-2 and *Ec*Hyd-3 (Pinske et al. 2012). Although these three membrane-bound hydrogenases have similar amino acid sequences, they are associated with different kinds of subunits (see below). Genomic annotation indicates the presence of a fourth hydrogenase although it has not been identified in the bacterium (Redwood et al. 2007). *Ec*Hyd-2 is a periplasmic membrane–bound hydrogenase, very active in hydrogen uptake (Dubini et al. 2002), that is expressed under microaerobic and anaerobic respiration. It transfers electrons resulting from H_2 oxidation to the (mena)quinone pool in the membrane, via its small subunit HybO, to the ferredoxin-like HybA subunit that contains four iron sulfur clusters and the intrinsic membrane subunit HybB devoid of metal (Dubini et al. 2002). These electrons are subsequently used in the reduction of fumarate to succinate on the cytoplasmic side of the membrane (Kröger et al. 2002). *Ec*Hyd-2 has a long anchoring α-helix, which corresponds to the C terminal segment of HybO. *Ec*Hyd-3 is part of the cytoplasmic, membrane–bound formate–hydrogenlyase complex consisting of seven different subunits, which catalyze the transformation of formate, a fermentation product, to CO_2 and H_2 (Leonhartsberger et al. 2002). This reaction prevents acidification of the bacterium cytoplasm and allows for hydrogen recycling. Whereas both *Ec*Hyd-2 and *Ec*Hyd-3 are very O_2-sensitive, *Ec*Hyd-1 is air-tolerant and oxidizes hydrogen at potentials significantly higher than those of

*Ec*Hyd-2 (Laurinavichene et al. 2002; Lukey et al. 2010). Amino acid sequence comparisons show that *Ec*Hyd-1 is related to membrane-bound hydrogenases (MBH) functioning in aerobic respiration in Knallgas bacteria. Like other enzymes from *E. coli*, *Ec*Hyd-1 is anchored to the membrane by a long trans–membrane α-helix from the small subunit and by an intrinsic membrane protein, cytochrome *b* (Dubini et al. 2002). The enzyme is a dimer of heterodimers (Volbeda et al. 2012), which are composed of a small and large subunit, i.e. a $(SL)_2$ dimer (Fig. 2.1b). Unlike MBH (but like *Ec*Hyd-3), *Ec*Hyd-1 is repressed by O_2 and highly expressed under fermentative growth (Pinske et al. 2012). Under these conditions the quinone pool is likely to be completely reduced, making a possible role of *Ec*Hyd-1 in anaerobic respiration difficult to rationalize. Indeed, experiments using *E. coli* mutants have shown that hydrogen produced by *Ec*Hyd-3 is mostly oxidized by *Ec*Hyd-2 and not by *Ec*Hyd-1 (Redwood et al. 2007). Consequently, *Ec*Hyd-1 and other O_2-tolerant enzymes could have a different function than respiration, such as defense against oxidative stress. This role has been proposed in the case of homoacetogenic bacteria living in termite guts (Boga and Brune 2003) and in the Fe(III)-reducing bacterium *Geobacter sulfurreducens* (Tremblay and Lovley 2012).

Most O_2-tolerant enzymes have significantly higher cluster redox potentials and much lower in vitro H_2 oxidation or production activities than the O_2-sensitive enzymes. High cluster potentials are probably beneficial for O_2 tolerance. In the following sections we will focus on the effects of O_2 on the structure and function of [NiFe]-hydrogenases, emphasizing the results obtained from crystallographic studies since 2001.

III. Structural Studies of O_2-Sensitive [NiFe]-Hydrogenases

Interpretation of the structural results obtained for [NiFe]-hydrogenases has been often complicated by the presence of mixtures of redox and protonation states in the crystals. This is due to the numerous redox states these enzymes display upon reduction from inactive oxidized to catalytically active species. In addition to O_2, molecules like H_2S, which can be present in significant amounts during the purification of enzymes from sulfate reducing bacteria, may react with the active site, producing another source of heterogeneity. Furthermore, the redox state of the structure may change depending on the X-ray dose used for collecting the crystallographic data. The different enzyme states have been extensively characterized by EPR and FTIR spectroscopic studies (De Lacey et al. 2007; Lubitz et al. 2007). Inactive oxidized states may be defined as unready and ready, which respectively give rise to EPR signals called Ni-A and Ni-B depending on whether they activate slowly or rapidly upon treatment with H_2. We obtained an almost pure Ni-B preparation from an active, anaerobically-purified periplasmic heterodimeric [NiFe]-hydrogenase of *Desulfovibrio (D.) fructosovorans* by exposing it to a mixture of 5 % H_2 and 95 % N_2 at pH 9.0 followed by exposure to a 100 % O_2 atmosphere at 0 °C. This sample was crystallized under air (Volbeda et al. 2005). The crystal structure showed the presence of spherical electron density between the Ni and Fe atoms of the active site that we assigned to a bridging hydroxide ligand (Fig. 2.3a). The crystallographic analysis of aerobically-purified enzyme in its "as-isolated" state showed a significantly more elongated electron density bridging the Ni and Fe ions (Fig. 2.3b). As aerobically purified enzyme is known to be mostly in the unready Ni-A state, we associated this observation with the presence of a peroxide species in this form. In addition, a small density feature close to a bridging cysteine thiol suggested its partial oxidation to a sulfenate (Volbeda et al. 2005). However, using data collected from a different crystal of "as isolated" enzyme, we observed spherical electron density bridging the Ni and Fe ions, as well as a small peak close to a bridging thiol. This crystal may have been overexposed to X-rays, as we also noticed the decarboxylation of several Asp and Glu

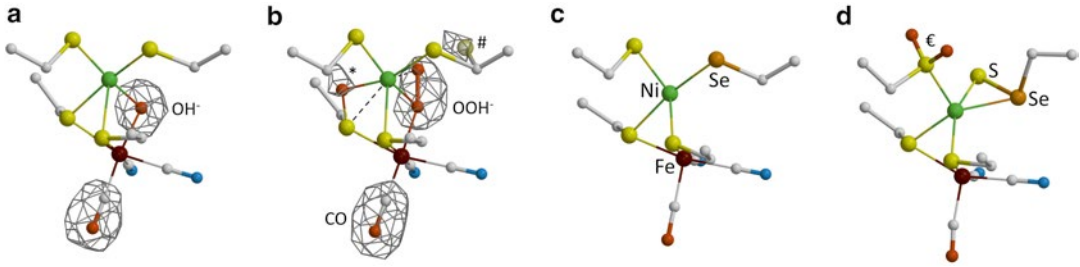

Fig. 2.3. Crystallographic models of the Ni-Fe(−Se) active site: (**a**) the ready Ni-B state in the *D. fructosovorans* enzyme; (**b**) the as-isolated, mainly unready mixture of the same enzyme; (**c**) the H_2-reduced [NiFeSe]-hydrogenase of *Desulfomicrobium baculatum*; (**d**) the major fraction of the as-isolated [NiFeSe]-hydrogenase of *D. vulgaris* Hildenborough. The gray grids in (**a**) and (**b**) depict an averaged omit electron density map, * denotes a partial oxidation of a Ni-Fe bridging thiolate ligand to a sulfenate, # an alternative conformation of a terminal Ni-bound thiolate and € a double oxidation of the other terminal Ni-bound thiolate to a sulfinate.

residues and the cleavage of a solvent-exposed disulfide bond (Volbeda et al. 2002). For the other crystals previously mentioned, there were no such signs of radiation damage.

The results described above may be explained as follows: active enzyme contains enough electrons in the active site and the [Fe-S] clusters to reduce O_2 completely, according to:

$$O_2 + 3H^+ + 4e^- \rightarrow H_2O + OH^- \qquad (2.1)$$

Two of the required electrons could come from a bridging hydride bound to either Ni(III)-Fe(II) (Ni-C) or Ni(II)-Fe(II) (Ni-R) in active enzyme (Brecht et al. 2003; Fontecilla-Camps et al. 2007; Pandelia et al. 2010) and the remaining two could be provided by reduced [Fe-S] clusters. One water molecule escapes the active site whereas the other one remains trapped as a bound hydroxide. During aerobic purification the initially reduced enzyme will gradually oxidize. However, the redox potentials for the Ni(II)/Ni(III) and $[Fe_3S_4]^+/[Fe_3S_4]^0$ cluster couples are positive enough to provide two electrons for O_2 reduction at the increasingly higher potentials encountered during enzyme purification:

$$O_2 + H^+ + 2e^- \rightarrow OOH^- \qquad (2.2)$$

The produced reactive peroxide species may oxidize thiolates to sulfenate (Forman et al. 2010), maybe after reduction of Ni(III) to Ni(II) because sulfenates are better ligands for the latter (Farmer et al. 1993):

$$Cys\text{-}S^- + OOH^- \rightarrow Cys\text{-}SO^- + OH^- \qquad (2.3)$$

Reaction (2.3), which also produces bound hydroxide, is thermodynamically very favorable (Söderhjelm and Ryde 2006). Consequently, it must have a rather large kinetic barrier in order to explain the predominant detection of the less stable peroxide intermediate. Our observations with the crystal overexposed to X-rays suggest that sulfenates may be further reduced to water and thiolate by photoelectrons produced by this radiation. Similar active site modifications have been reported for *D. vulgaris* Miyazaki (Ogata et al. 2005) and *Allochromatium (A.) vinosum* [NiFe]-hydrogenase (Ogata et al. 2010) in their "as-isolated" state. In the first case, a complicated mixture was observed including a partially occupied bridging peroxide, a partial modification of both a Ni-Fe bridging and a terminally Ni-bound thiolate to a sulfenate, and possibly, an additional fraction containing an inorganic sulfur ligand (S^{2-} or HS^-). In the second case, a spherical Ni-Fe bridging electron density was observed, along with a partial modification of a bridging

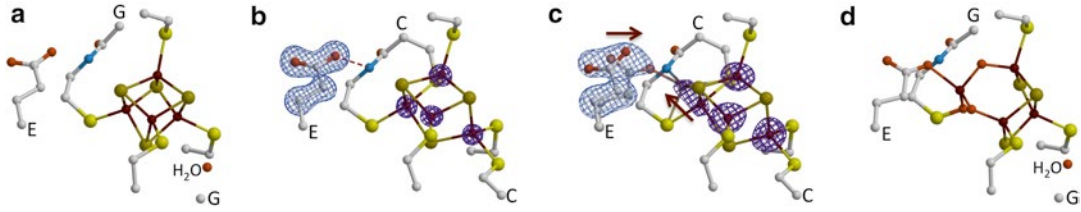

Fig. 2.4. Crystallographic models of the proximal iron-sulfur cluster: (**a**) $[Fe_4S_4]$-cluster in the *D. fructosovorans* enzyme, (**b**) $[Fe_4S_3]$-cluster in *E. coli* hydrogenase-1, observed in the H_2-reduced enzyme, (**c**) $[Fe_4S_3]$-cluster observed as a mixture of two states in as-isolated *E. coli* Hyd-1, (**d**) $[Fe_4S_3O_3]$-cluster observed in a fraction of the as-isolated *D. desulfuricans* ATCC 27,774 enzyme. Violet and blue grids denote anomalous difference and omit electron density maps.

thiolate to sulfenate. Using the data of our overexposed crystal of *D. fructosovorans* [NiFe]-hydrogenase and including quantum mechanical methods in the crystallographic refinement, Söderhjelm and Ryde (2006) obtained a similar result. This included a small fraction with a sulfenate modification of a bridging thiol (at a density peak that we had earlier attributed to noise) and an even smaller fraction with the Ni terminal thiolate ligand modified to sulfenate as observed by Ogata et al. (2005) in the *D. vulgaris* Miyazaki enzyme (although not exactly in the same conformation). In conclusion, although the exact identity of states like Ni-A and the one-electron more reduced unready Ni-SU form (Fig. 2.3b) is still debated, our interpretations seem to be compatible with all the discussed crystallographic, as well as with other experimental results, as previously reviewed by Fontecilla-Camps et al. (2007). Besides reacting at the active site, O_2 may also react with and presumably damage Fe-S clusters, as exemplified by the partial conversion of the proximal $[Fe_4S_4]$ to a $[Fe_4S_3O_3]$ cluster observed in the crystal structures of *D. desulfuricans* ATCC 27774 [NiFe]-hydrogenase (Matias et al. 2001) (Fig. 2.4d) and *D. vulgaris* Hildenborough [NiFeSe]-hydrogenase (Marques et al. 2010).

In theory there are at least three ways to decrease the oxygen sensitivity of a [NiFe]-hydrogenase: (A) to limit the access of O_2 to the active site, (B) to speed up the activation of oxidized states and (C) to avoid the formation of reactive oxygen species according to reactions (2.2) and (2.3) by keeping enough electrons available for the complete reduction of O_2 to water. Studies with mutants have shown that strategy A, which limits oxygen access through the tunnel connecting the active site to the protein exterior (Montet et al. 1997) may indeed explain the O_2-tolerance of H_2 sensors, also called regulatory hydrogenases (Buhrke et al. 2005; Duche et al. 2005). This possibility was predicted from sequence alignments with O_2-sensitive hydrogenases (Volbeda et al. 2002). However, the function of these sensors is to activate the synthesis of hydrogenases when hydrogen is present by interacting with a histidine protein kinase, which in turn, modulates the activity of a response regulator-transcription factor (Elsen et al. 2003; Buhrke et al. 2004). As hydrogenases they have very little activity. We will not review the elegant studies carried out with mutants of the tunnel and other regions using the O_2-sensitive periplasmic *D. fructosovorans* [NiFe]-hydrogenase as they are described in Chap. 3 of this book. Instead, we will next discuss those enzymes that are either naturally O_2-resistant or O_2-tolerant by using strategies B and C, respectively.

IV. Structural Studies of O_2-Resistant [NiFeSe]-Hydrogenases

In some [NiFe]-hydrogenases, one of the cysteine ligands of the Ni is naturally substituted by a seleno-cysteine (SeCys) and, in addition, the mesial $[Fe_3S_4]$ is replaced by a

$[Fe_4S_4]$ cluster. In general, as recently reviewed by Baltazar et al. (2011), such [NiFeSe]-hydrogenases have much higher catalytic activity than the [NiFe] enzymes and they often appear to be less O_2-sensitive. The crystal structure of [NiFeSe]-hydrogenase from the sulfate reducing bacterium *Desulfomicrobium baculatum*, was reported by Garcin et al. (1999). It was both the first structure determined for this class of hydrogenase and one of the first, together with the structure reported by Higuchi et al. (1999) for *D. vulgaris* Miyazaki [NiFe]-hydrogenase, with a reduced active site, probably in the Ni-C state (Fig. 2.3c). Based on several sources (Brecht et al. 2003; Fontecilla-Camps et al. 2007; Pandelia et al. 2010), a hydride is postulated to bridge the Ni and Fe ions in the active Ni-C form, replacing the hydroxide found in the Ni-B state. More recently, Marques et al. (2010) have reported on the structure of the [NiFeSe]-hydrogenase from *D. vulgaris* Hildenborough. This structure contains a mixture of oxidized states and includes three different conformations for its SeCys residue. Quite unexpectedly, about 70 % of the structure appears to contain a doubly oxidized thiol (a sulfinate) and a persulfurated SeCys (Fig. 2.3d). Assuming it contains Ni(II), which is reasonable given the absence of EPR signals from oxidized [NiFeSe]-hydrogenase preparations, this highly oxidized active site will require no less than seven electrons and up to seven protons to be converted into the reduced Ni-C state (Fig. 2.3c): two electrons will be needed to reduce the Se-S bond, producing either H_2S or HS^-; four additional electrons will be required to reduce the two S-O bonds, producing two H_2O molecules, and one more electron must be employed, along with the oxidation of Ni(II) to Ni(III), to reduce a proton and generate the hydride. It is difficult to reconcile such a highly oxidized structure with the inherent O_2-resistance of [NiFeSe]-hydrogenases, because sulfinates are thermodynamically very stable hyperoxidized species that normally require dedicated enzymes for their reduction (Poole and Nelson 2008). Consequently, we conclude that additional studies, including structures of intermediate oxidation states, will be required to understand how the structure reported by Marques et al. (2010) could be generated and to determine whether it is easily activated. These studies should also shed light on the role of SeCys in activation and O_2 resistance. One possible reason for the SeCys/Cys substitution in these enzymes is the fact that Se-O bonds that might be formed upon air exposure are inherently weaker than S-O bonds (Parkin et al. 2008) and, consequently, easier to break.

V. Structural Studies of O_2-Tolerant Membrane-Bound [NiFe]-Hydrogenases

Amino acid sequence comparisons (Pandelia et al. 2012) have shown that a family of oxygen-tolerant hydrogenases has two supernumerary small subunit cysteine residues in the coordination sphere of the proximal cluster (Figs. 2.4a, b). These enzymes can oxidize hydrogen at the 21 % atmospheric oxygen level. As first shown in the case of *Aquifex aeolicus* hydrogenase 1 (*Aa*Hyd-1), the proximal cluster (PC) is involved in two one–electron redox process, involving PC1/PC2 (formal +1/+2) and PC2/PC3 (formal +2/+3) states. The higher potential PC2/PC3 redox transition does not change between pH 6.4 and 7.4. Other adaptations for their tolerance to oxygen are (i) a lower K_m for H_2 than the K_I for O_2 and (ii) the fact that all the metal centers have more positive potentials when compared to oxygen–sensitive NiFe hydrogenases. It has been shown that the superoxidized proximal cluster has more ferric character than standard clusters (Pandelia et al. 2011). This observation agrees with the proposition that the two oxidation steps of the proximal cluster correspond to 3Fe(II)-1Fe(III) → 2Fe(II)-2Fe(III) and 2Fe(II)-2Fe(III) → 1Fe(II)-3Fe(III) changes (Goris et al. 2011; Pandelia et al. 2011) in the PC1/PC2 and PC2/PC3 redox couples, respectively. It is noteworthy that these two redox couples are separated by a narrow potential

difference of about 0.2 V (see also Roessler et al. 2012), compared to others, such as the one of high potential iron sulfur protein, where the unnatural super-reduction from $[Fe_4S_4]^{+2}$ to $[Fe_4S_4]^{+1}$ involves a much higher potential drop of 1 V relative to the +3/+2 redox couple (Heering et al. 1995). The structures of three oxygen-tolerant hydrogenases have been published including one solved by us (Fritsch et al. 2011b; Shomura et al. 2011; Volbeda et al. 2012). These studies have shown that the proximal cluster has an unusual structure where the supernumerary Cys19 bridges two iron ions and Cys120 terminally binds another one. Thus, these two cysteine residues replace a sulfide ligand. Site–directed mutagenesis has shown that the supernumerary Cys19 is crucial for oxygen tolerance whereas the supernumerary Cys120 plays a less important role (Lukey et al. 2011). The proximal cluster displays a remarkable plasticity undergoing a major conformational change when it goes from the PC2 to the PC3 state. This change involves the migration of one of the iron ions of the cluster towards the amide N of Cys20 forming a bond with it (Fig. 2.4c). In addition, this iron ion now binds the carboxylate group of a glutamate residue. An equivalent glutamate also binds the corresponding iron in oxygen-damaged proximal clusters (Fig. 2.4d). We have used our *Ec*Hyd-1 structure (Volbeda et al. 2012) to calculate and reproduce previously generated Mössbauer and EPR spectroscopic data using *Aa*Hyd-1. Our calculations show that the amide–N deprotonation, required to form the Fe-N bond, is mediated by the carboxylate group of the glutamic acid mentioned above. This residue is hydrogen-bonded to another glutamate residue, which is part of a proton transfer chain that normally operates by moving protons from the active site to the molecular surface (Fontecilla et al. 2007; Fdez Galván et al. 2008). However, when exposed to oxygen, the enzyme operates in the opposite direction by sending both protons and electrons to the active site. Under normal anaerobic conditions hydrogen uptake makes the cluster oscillate between PC1 and PC2, like in oxygen-sensitive hydrogenases. However, when the enzyme is exposed to O_2, and if the active site is in the Ni–C state with bound hydride, oxygen will be reduced to peroxide. In order to avoid subsequent oxidative damage this species has to be rapidly reduced to water. As mentioned above, this is mediated by the proximal cluster, which goes from PC1 to PC3 in two rapid successive one–electron reduction steps. Evidence for a water channel close to the active site has been also obtained from our structure. This channel is essential for evacuating the water generated upon oxygen reduction to the molecular surface. Our calculations show that the unique iron that forms a bond with the N amide atom of Cys20 is the one that gets oxidized from ferrous to ferric when the cluster goes from PC2 to PC3. Our conclusion is that if the active site stays in the Ni-B state and in the absence of H_2, there will not be electrons available to reduce the proximal cluster from the PC3 to the PC2 and PC1 state. Thus, both the Ni-B form and the superoxidized proximal cluster in the PC3 state protect the integrity of the hydrogenase when exposed to molecular oxygen. From a biotechnological standpoint these hydrogenases have potential applications in bio-fuel cells (see below). Conversely, and because of their more positive redox potentials relative to standard hydrogenases, these enzymes cannot be effectively used for hydrogen evolution.

*Ec*Hyd-1 is naturally bound to the periplamic side of the cytoplasmic membrane. It forms a dimer of heterodimers bringing the two distal clusters within 12 Å (Fig. 2.1b), a distance compatible with fast electron transfer (Page et al. 2003). So, it is possible to postulate that electrons generated at the active site of one monomer could be transferred to the active site of the other, i.e. the active site of one of the enzymes could help jumpstarting the other (Volbeda et al. 2012). This arrangement lowers the probability of the simultaneous oxygen-induced deactivation of the two hydrogenases in the dimer. Frielingsdorf et al. (2011) have proposed a trimeric arrangement for the heterodimers of

the oxygen–tolerant *Re*MBH. We have modeled such a trimer and found that the distance between two distal clusters is too large to allow for efficient electron transfer. Furthermore, amino acid sequence comparisons for regions involved in monomer–monomer recognition indicate that they are well conserved in *Ec*Hyd-1 and *Re*MBH (not shown). This strongly suggests that *Re*MBH also forms a dimer of heterodimers. Furthermore, the same oligomeric state has been found in other hydrogenases, both of the O_2–sensitive and O_2–tolerant kinds, such as those from *Allochromatium vinosum* (Ogata et al. 2010) and *Hydrogenovibrio marinus* (Shomura et al. 2011), respectively.

VI. Regulation of Hydrogenase Expression and Activity: The Example of *Escherichia coli*

In order to elucidate the regulation and role of the three well-characterized H_2ases in *E. coli* one has to look into its fluctuating lifecycle from the moment it is ingested to the moment it is excreted by the host. Alexeeva et al. (2002) have put forward the concept of perceived aerobiosis that is defined as the extent to which the bacterium will use oxidative catabolism. At over 50 % aerobiosis, *E. coli* respires O_2 using low-affinity cytochrome *bo* oxidase. Conversely, below 40 % aerobiosis, the high-affinity cytochrome *bd-I* oxidase is expressed, upregulated by ArcA, the anoxic redox control regulator (Alexeeva et al. 2000). Under these conditions, cytochrome *bd-I* oxidase becomes the major terminal oxygen reductase and, thanks to its activity the intracellular oxygen tension is kept low enough to allow for, (i) pyruvate–formate lyase activity, which generates formate from pyruvate, and (ii) protection of the bacterium from oxidative damage induced by dyes (Alvarez et al. 2010). At lower oxygen concentrations, cytochrome *bd-I* oxidase expression is repressed by the fumarate-nitrate reduction regulator (FNR). FNR is a transcriptional regulator of respiratory pathway genes that becomes activated at 0.5 % O_2 when *E. coli* goes from microaerobic to anaerobic growth conditions (Becker et al. 1996). Anaerobic conditions cause the expression of an additional cytochrome oxidase called *bd-II,* which is co-regulated with the expression of the O_2-tolerant *Ec*Hyd-1 (Dassa et al. 1991). As *bd-I, bd-II* has high affinity for oxygen and is well suited to function in an anaerobic environment. In microorganisms such as *Azotobacter vinelandii*, which possess the highly oxygen–sensitive, nitrogen-reducing nitrogenase, high-affinity cytochrome oxidases afford protection against oxygen–induced damage (Poole and Hill 1997). The physiological role of *Ec*Hyd-1 has not been clearly determined. Most in vitro experiments are not well suited to clarify this point because one has to look at the natural environment where this bacterium grows in order to understand when and why the three different H_2ases are expressed. *Ec*Hyd-1 expression is upregulated under stressful conditions such as carbon and phosphate starvation, osmotic shock, and stationary phase conditions (Atlung et al. 1997) and both *Ec*Hyd-1 and *Ec*Hyd-3 are highly expressed under fermentative conditions, i.e., their expression is stimulated by formate (Brøndsted and Atlung 1994). These conditions are naturally found in the anoxic terminal segment of the gastro–intestinal tract of the host. The role of *Ec*Hyd-3 in recycling hydrogen and preventing acidification of the cytoplasm according to the reaction:

$$HCOO^- + H^+ \rightarrow CO_2 + H_2 \qquad (2.4)$$

is well established. But, in the case of *Ec*Hyd-1 it is not easy to explain why an oxygen-tolerant H_2ase is highly expressed under fermentative conditions when there is excess of reducing equivalents and electron acceptors are scarce (except for endogenously produced fumarate) (Pinske et al. 2012). Furthermore, because under these conditions the quinone pool should be fully reduced, it would make little sense to generate additional electrons from hydrogen oxidation. Conversely, the enzyme will very

rapidly reduce any traces of oxygen present in the periplasmic space. This is so because, under these conditions, O_2 will constitute the only sink for H_2-generated electrons. As discussed above, our crystal structure (Fig. 2.1b) and electron transfer rate calculations favor direct oxygen reduction to water as the main activity of this enzyme when anaerobic *E. coli* is exposed to this gas, according to the Knallgas reaction:

$$O_2 + 2H_2 \rightarrow 2H_2O \qquad (2.5)$$

As long as there is H_2 being produced by *Ec*Hyd-3 from formate, *Ec*Hyd-1 will oxidize it and use the resulting electrons to reduce O_2 if any is present.

Several experiments have shown that *Ec*Hyd-1 cannot reduce low-potential artificial electron acceptors (Pinske et al. 2011). The enzyme, however, is capable of reducing nitroblue tetrazolium (NBT), a redox dye with E_0'=−80 mV (Pinske et al. 2012). This activity does not require the presence of the cognate membranous cytochrome *b*, indicating that the reduction is performed directly by the H_2ase. The catalytic bias of *Ec*Hyd-1 to hydrogen oxidation is related to its oxygen tolerance. Indeed, it has been shown that this enzyme has an overpotential of about +50 mV when compared to *Ec*Hyd-2 (Lukey et al. 2010). This overpotential also implies that the activity/inactivity switch of *Ec*Hyd-1 is shifted to higher potentials than in the case of *Ec*Hyd-2. Conversely, this over-potential prevents *Ec*Hyd-1 from being able to reduce protons or low–potential dyes (Lukey et al. 2010; Pinske et al. 2011).

The role of *Ec*Hyd-2 and the regulation of its expression are easier to rationalize. This enzyme, which resembles H_2ases from sulfate–reducing bacteria in terms of its catalytic properties, is expressed under microaerobic and anaerobic conditions. Its physiological role is hydrogen uptake (Dubini et al. 2002). *Ec*Hyd-2 can use fumarate as electron acceptor and its expression correlates with fumarate respiration (Pinske et al. 2012). Conversely, nitrate is a repressor of the expression of this enzyme. *Ec*Hyd-2 shows low benzyl viologen (BV) reduction activity in cell extracts. By comparison, *Ec*Hyd-3 is very effective in reducing this dye, which, although not biologically relevant, is related to the potentials at which this enzyme functions in proton reduction (Pinske et al. 2011).

VII. [NiFe]-Hydrogenase Maturation

The biosynthesis of the Ni-Fe active site is a complex energy-consuming and species-specific process. Moreover, when there are several hydrogenases in the same species, each of them has its own maturation machinery. In the extensively studied biosynthetic pathway of *Ec*Hyd-3 (Böck et al. 2006) at least ten gene products are involved. The cyanide precursor $H_2NC(O)P_i$ (carbamoylphosphate, here abbreviated CP) is produced by CP-synthetase from L-glutamine and bicarbonate in reactions 1–3 (Scheme 2.1), with concomitant consumption of two ATP molecules (Thoden et al. 1997). CP is converted by *HypF* to $H_2NC(O)$-AMP, also in an ATP-dependent reaction (reactions 4–5). After formation of a *HypEF* complex, of known structure (Shomura and Higuchi 2012), the H_2NCO group is transferred to the C-terminal cysteine of HypE (reaction 6). The resulting thiocarbamate is subsequently dehydrated in yet another ATP-dependent reaction to thiocyanate (reaction 7), followed by CN transfer to Fe bound to *HypCD* (reaction 8) in a putative *HypCDE* complex (Watanabe et al. 2007). Reactions 1–8 are repeated for the transfer of a second CN ligand to Fe, whereas CO is provided by a so far unknown donor (Bürstel et al. 2011) in reaction 9. The resulting $FeCO(CN)_2$ moiety is next transferred to *apo-pre-HycE* (reaction 10), followed by a SlyD-dependent Ni transfer (Chung and Zamble 2011; Kaluarachchi et al. 2012) from the GTPase *HypB* (reaction 11). Maturation is finished by the cleavage of a short C-terminal peptide of *pre-HycE* (reaction 12) by the endopeptidase *HycI*. The Ni insertion machinery further involves Ni transfer to *HypB* from the *HypA* carrier (reaction 15), which itself is charged with Ni

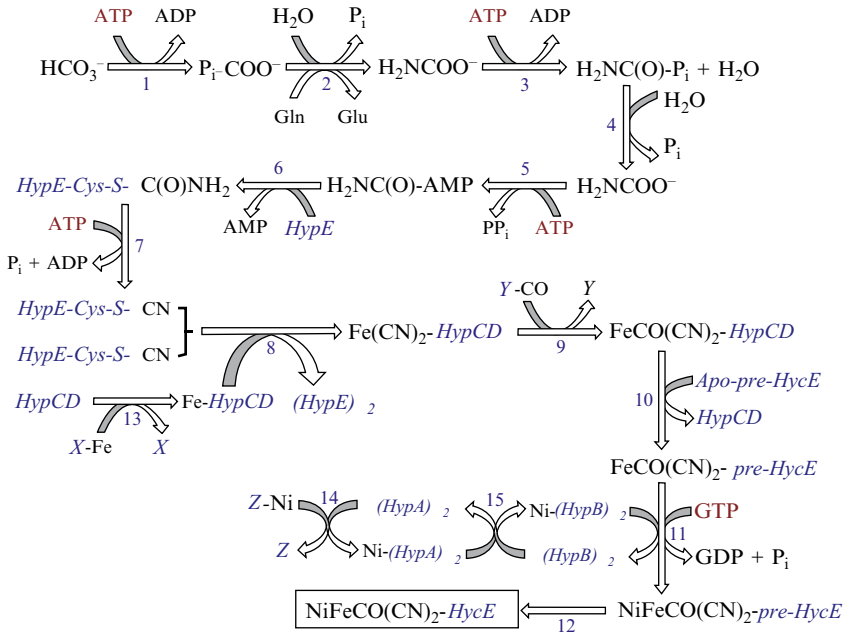

Scheme 2.1. Maturation of the Ni-Fe-containing HycE subunit of *Ec*Hyd-3. The enzymes/proteins involved, with reactions numbered 1–15, are carbamoylphosphate synthetase (1–3), *HypF* (4–7), *HypE* (7–8), *HypC and HypD* (8–10, 13), HypB and *SlyD* (11, 15), *HycI* (12) and *HypA* (14–15). *X, Y* and *Z* are unknown donors of Fe, CO and Ni, respectively.

by an unknown donor (reaction 14). The donor of Fe to *HypCD* (reaction 10) is also unknown. Taking all the reactions into account, at least eight ATP molecules and one GTP are required to complete the active site maturation. However, given the incomplete characterization of the pathways for metal transfer and production of the CO ligand, the actual energy requirements could be significantly higher.

Significant insight into the molecular aspects of the *Ec*Hyd-3 large subunit maturation has been provided by the X-ray structure determinations of *HypA*, *HypB*, *HypC*, *HypD*, *HypE*, *HypF*, *HycI* and *SlyD* (Watanabe et al. 2009; Xia et al. 2009; Gasper et al. 2006; Chan et al. 2012; Watanabe et al. 2007; Shomura et al. 2007; Rangarajan et al. 2008; Shomura and Higuchi 2012; Petkun et al. 2011; Kumarevel et al. 2009; Loew et al. 2010), but some details remain unclear. In addition, although *apo-pre-HycE* has been generally assumed to be devoid of metal, a recent report suggests that a mutant of *HybC*, the homologous unprocessed large subunit of *Ec*Hyd-2, may actually contain a labile [Fe_4S_4] cluster at the active site position in the mature subunit (Soboh et al. 2012). If this were also the case for the native, unprocessed subunit, an additional step would be needed involving removal of the cluster, before incorporation of the Ni-Fe site.

An interesting aspect is the sensitivity of the maturation process towards oxygen. In the maturation of the O_2-tolerant *Re*MBH, extra gene products are involved that allow production of active enzyme under aerobic conditions (Fritsch et al. 2011a). The same applies to *Se*Hyd-5, the homologous O_2-tolerant hydrogenase-5 of *Salmonella enterica* serovar Typhimurium (Parkin et al. 2012). However, the latter organism also produces an O_2-tolerant Hyd-1 that, like the related *Ec*Hyd-1 enzyme, is only expressed under anoxic conditions. The maturation of these enzymes is most likely O_2-sensitive, because it does not involve gene products related to those used

for *Re*MBH and *Se*Hyd-5 maturation, under air. In conclusion, aerobic production of O_2-tolerant [NiFe]-hydrogenases requires O_2-tolerant maturation.

VIII. Biotechnological Applications

Using electrochemistry, Vincent and collaborators (2005a, b, 2007) have studied mechanisms of catalysis, electron transfer, activation and inactivation, and defined important properties such as O_2 tolerance and CO resistance of H_2ases in physical terms. These enzymes are alternatives to noble metals for the production of hydrogen from solar energy (Jones et al. 2002). The latter are nonselective and can be poisoned by environmental pollutants whereas the enzymes are highly specific and relatively resistant. Like Pt, H_2ases produce hydrogen with minimal overpotential and are catalytically very efficient. For that reason, these enzymes are promising targets for developing new catalysts with biotechnological applications.

A. Membrane-Bound [NiFe]-Hydrogenase

The oxygen–tolerant hydrogenase from *Ralstonia metallidurans* CH34 and the fungal O_2-reductase laccase have been adsorbed to graphite electrodes to build an open bio–fuel cell that could generate electricity from 3 % hydrogen, under normal atmospheric conditions and in aqueous solution (Vincent et al. 2005a, 2006). This setup was shown to be capable of powering a wristwatch for several hours. Although the hydrogenase had to be activated after a few hours, this experiment has opened the possibility of powering electronic devices using low hydrogen concentrations in air. Because of the very high specificity of the enzymes, which is not the case of Pt that catalyzes both the anodic and cathodic sides of the reaction, no costly membrane is required in the fuel cell setup (Fig. 2.5a).

B. [NiFeSe]-Hydrogenase

Reisner et al. (2009) and Reisner and Armstrong (2011) have carried out a systematic study of enzyme efficiency by coupling colloidal semi-conductor TiO_2 nanoparticles with a synthetic ruthenium photosensitizer to different H_2ases. When a H_2ase is attached to an n-type semiconducting surface, rather than to a metallic or semi-metallic material like graphite, the direction of catalysis can be altered with a bias towards reduction reactions. This is convenient in the case of hydrogen production. The work by Reisner et al. is a proof of concept: the dye injects an electron into the conduction band of TiO_2 when exposed to visible light. This, in turn, oxidizes the dye and reduces TiO_2, which transfers electrons directly to the adsorbed H_2ase that reduces protons to molecular hydrogen. A sacrificial electron donor reduces the dye, closing the cycle (Fig. 2.5b). Reisner et al. (2009) and Reisner and Armstrong (2011) concluded that the most efficient available system included the [NiFeSe]-H_2ase from *Dm. baculatum* and the tris(bipyridyl) ruthenium photosensitizer RuP. The latter fulfills several requirements including (1) an absorption band in the visible spectrum, (2) stable attachment to TiO_2, (3) efficient charge separation and (4) long-term stability upon irradiation. Conversely, the choice of *Dm. baculatum* H_2ase was determined by several factors: (1) it has good hydrogen production activity; (2) it can be rapidly reactivated at low potentials after O_2–induced inactivation; (3) it can operate in the presence of about 1 % O_2 and (4), there is significant proton reduction even at 5 % H_2, which is usually inhibitory to H_2ases. However, these characteristics are not enough to render a H_2ase optimal for hydrogen production. A simple calculation indicates that the distal [Fe_4S_4] cluster of *Dm. baculatum* H_2ase is surrounded by a negatively charged surface patch. Thus, the interaction between the enzyme and the TiO_2 particle is mostly controlled by localized polar interactions rather than overall electrostatic interactions. As a conclusion, the

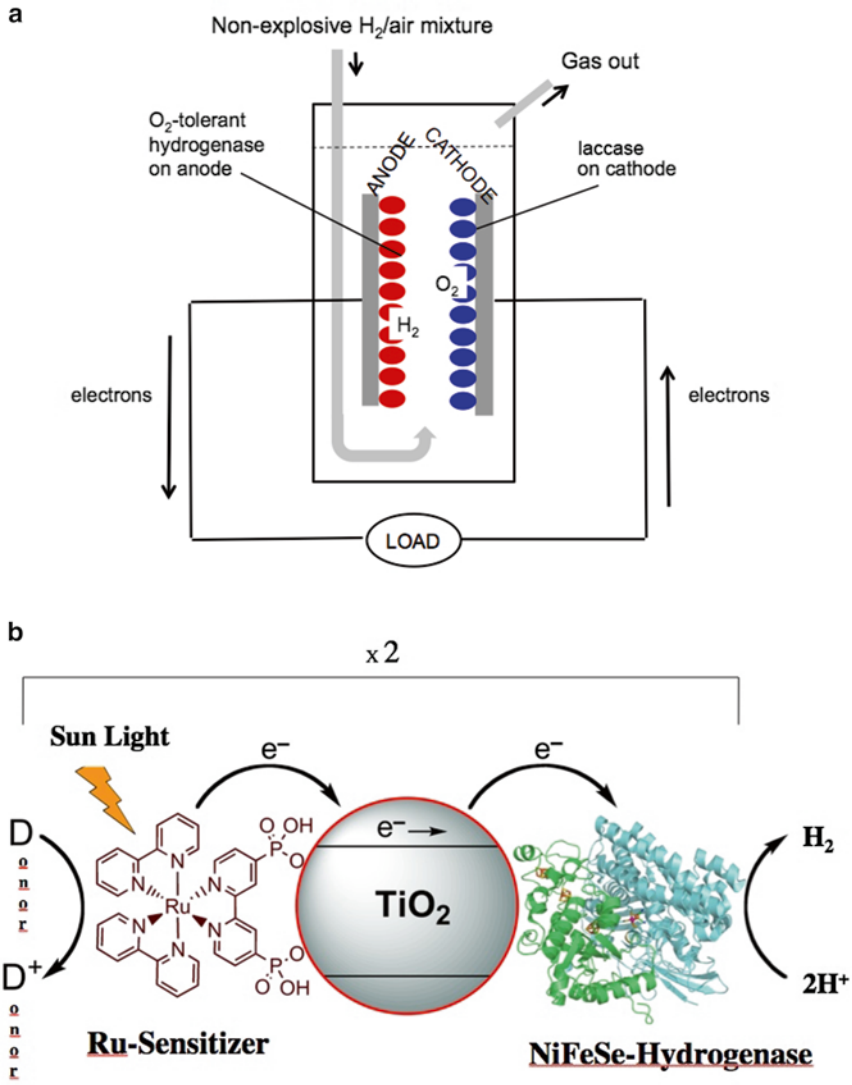

Fig. 2.5. (**a**) A bio-fuel cell comprising a graphite cathode modified with high potential fungal laccase and a graphite anode modified with the O_2-tolerant membrane-bound hydrogenase of *Ralstonia metallidurans* CH34 in aqueous electrolyte under an atmosphere of 3 % H_2 in air (Adapted from Vincent et al. 2005a); (**b**) Schematic representation of visible-light driven H_2 evolution with [NiFeSe]-H_2ase attached to RuP dye sensitized TiO_2 nanoparticles. Excitation by visible light in the presence of a sacrificial electron donor (Donor), causes RuP to inject an electron into the conduction band of the semi-conductor TiO_2. The electrons, which are transferred directly to the adsorbed [NiFeSe]-H_2ase, reduce H^+ from the buffered aqueous solution generating H_2. The three [Fe_4S_4]-clusters (indicated in the figure) form a "wire" responsible for electron transfer to and from the active site of the [NiFeSe]-H_2ase. The structure of the sensitiser RuP is also shown (*left side*). Two cycles are required to generate a H_2 molecule (Adapted from Reisner et al. 2009).

authors found that *Dm. baculatum* H_2ase has the very well suited property of being titaniaphilic. Taken together, these results should play an important role in the future design and assembly of robust H_2ase-nanoparticle devices including mesoporous 3D electrodes for enzyme–fuel cells or biosensors. The production of hydrogen at room temperature from neutral water without redox–mediators represents a significant

step towards the development of an artificial system mimicking photosynthetic green algae. In a related approach, Lubner et al. (2010) have connected photosystem I (PS I) and an [FeFe]-H_2ase and have assayed electron transfer between the two components via light-induced H_2 generation.

C. Bio-inspired Artificial Hydrogen Catalysts

Helm et al. (2011) have reported on which may be the most efficient bio-inspired catalyst synthesized so far. It is the synthetic nickel complex, $[Ni(P(Ph)_2N(Ph)_2)](BF_4)_2$, $(P(Ph)_2N(Ph)) = 1,3,6$-triphenyl-1-aza-3,6-diphosphacycloheptane, which catalyzes the production of H_2 with protonated dimethylformamide as the proton donor. Turnover frequencies of 106,000 per second have been obtained in the presence of 1.2 M of water. This remarkably fast catalyst combines features of the two major types of H_2ases: a Ni ion ([NiFe]-H_2ase) and pendant amines that function as proton relays ([FeFe]-H_2ases). A computational study on a related compound suggests that proton transfers between the amine nitrogen and the nickel are favored relative to a direct nitrogen-to-nitrogen proton transfer (O'Hagan et al. 2011). This result supports our proposition that the bridgehead atom of the thiolate-containing small molecule at the [FeFe]-H_2ase active site is nitrogen (Nicolet et al. 2001).

IX. Conclusions

The structural studies of [NiFe]-H_2ases have shed considerable light on the catalytic mechanism of hydrogen uptake and proton reduction. Both processes are of biotechnological interest and are the subject of very active research. One major goal in this field is the coupling of solar energy to hydrogen production. The O_2-resistant [NiFeSe]-H_2ase has proven to be a very effective H_2 producer thanks to its very high affinity for TiO_2 particles. Another promising domain is the use of the O_2-tolerant enzymes in bio-fuel cells although the relative fragility of these molecules limits their application at present time. Maybe more importantly, the active sites of hydrogenases have inspired the synthesis of novel catalysts with very good performances. In addition, structural strategies such as the one employed by the $[Fe_4S_3]$ cluster of the O_2-tolerant [NiFe]-H_2ases, which is capable of two-electron redox chemistry, should also inspire new ways of designing synthetic catalysts for hydrogen oxidation.

Acknowledgements

The authors thank the Commissariat à l'Energie Atomique et aux Energies Alternatives (CEA) and the Centre National de la Recherche Scientifique (CNRS) for institutional funding and the Agence Nationale de la Recherche for several contracts concerning the subject of this chapter. Erwin Reisner is thanked for providing Fig. 2.5b.

References

Alexeeva S, de Kort B, Sawers G, Hellingwerf KJ, de Mattos JT (2000) Effects of limited aeration and of the ArcAB system on intermediary pyruvate catabolism in *Escherichia coli*. J Bacteriol 182:4934–4940

Alexeeva S, Hellingwerf KJ, de Mattos JT (2002) Quantitative assessment of oxygen availability: perceived aerobiosis and its effect on flux distribution in the respiratory chain of *Escherichia coli*. J Bacteriol 184:1402–1406

Alvarez AF, Malpica R, Contreras M, Escamilla E, Georgellis D (2010) Cytochrome *d* but not cytochrome *o* rescues the toluidine blue growth sensitivity of arc mutants of *Escherichia coli*. J Bacteriol 192:391–399

Atlung T, Knudsen K, Heerfordt L, Brøndsted L (1997) Effects of sigmaS and the transcriptional activator AppY on induction of the *Escherichia coli* hya and cbdAB-appA operons in response to carbon and phosphate starvation. J Bacteriol 179:2141–2146

Baltazar CSA, Marques MC, Soares CM, DeLacey AM, Pereira IAC, Matias PM (2011) Nickel–iron–selenium hydrogenases – an overview. Eur J Inorg Chem 2011:948–962

Becker S, Holighaus G, Gabrielczyk T, Unden G (1996) O_2 as the regulator signal for FNR-dependent

gene regulation in *Escherichia coli*. J Bacteriol 178:4515–4521

Böck A, King PW, Blokesch M, Posewitz MC (2006) Maturation of hydrogenases. Adv Microb Physiol 51:1–71

Boga HI, Brune A (2003) Hydrogen-dependent oxygen reduction by homoacetogenic bacteria isolated from termite guts. Appl Environ Microbiol 69:779–786

Bothe H, Schmitz O, Yates MG, Newton WE (2010) Nitrogen fixation and hydrogen metabolism in cyanobacteria. Microbiol Mol Biol Rev 74:529–551

Brecht M, Van Gastel M, Buhrke T, Friedrich B, Lubitz W (2003) Direct detection of a hydrogen ligand in the [NiFe] center of the regulatory H_2-sensing hydrogenase from *Ralstonia eutropha* in its reduced state by HYSCORE and ENDOR spectroscopy. J Am Chem Soc 125:13075–13083

Brøndsted L, Atlung T (1994) Anaerobic regulation of the hydrogenase 1 (*hya*) operon of *Escherichia coli*. J Bacteriol 176:5423–5428

Buhrke T, Lenz O, Porthun A, Friedrich B (2004) The H_2-sensing complex of *Ralstonia eutropha*: interaction between a regulatory [NiFe] hydrogenase and a histidine protein kinase. Mol Microbiol 51:1677–1689

Buhrke T, Lenz O, Krauss N, Friedrich B (2005) Oxygen tolerance of the H_2-sensing [NiFe] hydrogenase from *Ralstonia eutropha* is based on limited access of oxygen to the active site. J Biol Chem 280:23791–23796

Bürstel I, Hummel P, Siebert E, Wisitruangsakul N, Zebger I, Friedrich B, Lenz O (2011) Probing the origin of the metabolic precursor of the CO ligand in the catalytic center of [NiFe] hydrogenase. J Biol Chem 286:44937–44944

Chan K-H, Li T, Wong C-O, Wong K-B (2012) Structural basis for GTP-dependent dimerization of hydrogenase maturation factor HypB. PLoS One 7:e30547

Chung KC, Zamble DB (2011) The Escherichia coli metal-binding chaperone SlyD interacts with the large subunit of [NiFe]-hydrogenase 3. FEBS Lett 585:291–294

Dassa J, Fsihi H, Marck C, Dion M, Kieffer-Bontemps M, Boquet PL (1991) A new oxygen-regulated operon in *Escherichia coli* comprises the genes for a putative third cytochrome oxidase and for pH 2.5 acid phosphatase (*appA*). Mol Gen Genet 229:341–352

De Lacey AL, Fernández VM, Rousset M, Cammack R (2007) Activation and inactivation of hydrogenase function and the catalytic cycle: spectroelectrochemical studies. Chem Rev 107:4304–4330

Dubini A, Pye RL, Jack RL, Palmer T, Sargent F (2002) How bacteria get energy from hydrogen: a genetic analysis of periplasmic hydrogen oxidation in *Escherichia coli*. Int J Hydrog Energy 27: 1413–1420

Duché O, Elsen S, Cournac L, Colbeau A (2005) Enlarging the gas access channel to the active site renders the regulatory hydrogenase HupUV of *Rhodobacter capsulatus* O_2 sensitive without affecting its transductory activity. FEBS J 272:3899–3908

Efremov RG, Sazanov LA (2012) The coupling mechanism of respiratory complex I – a structural and evolutionary perspective. Biochim Biophys Acta 1817:1785–1795

Elsen S, Duché O, Colbeau A (2003) Interaction between the H_2 sensor HupUV and the histidine kinase HupT controls HupSL hydrogenase synthesis in *Rhodobacter capsulatus*. J Bacteriol 185:7111–7119

Farmer PJ, Reibenspies JH, Lindahl PA, Darensbourg M (1993) Effect of sulfur site modification on the redox potentials of derivatives of [N, N'-bis(2-mercaptoethyl)-1,5-diazocyclooctanato]nickel(II). J Am Chem Soc 115:4665–4674

Fdez Galván I, Volbeda A, Fontecilla-Camps JC, Field MJ (2008) A QM/MM study of proton transport pathways in a [NiFe] hydrogenase. Proteins 73:195–203

Fontecilla-Camps JC, Volbeda A, Cavazza C, Nicolet Y (2007) Structure/function relationships of [NiFe]- and [FeFe]-hydrogenases. Chem Rev 107:4273–4303

Forman HJ, Maiorino M, Ursini F (2010) Signaling functions of reactive oxygen species. Biochemistry 49:835–842

Frielingsdorf S, Schubert T, Pohlmann A, Lenz O, Friedrich B (2011) A trimeric supercomplex of the oxygen-tolerant membrane-bound [NiFe]-hydrogenase from *Ralstonia eutropha* H16. Biochemistry 50:10836–10843

Fritsch J, Lenz O, Friedrich B (2011a) The maturation factors HoxR and HoxT contribute to oxygen tolerance of membrane-bound [NiFe] hydrogenase in *Ralstonia eutropha* H16. J Bacteriol 193:2487–2497

Fritsch J, Scheerer P, Frielingsdorf S, Kroschinsky S, Friedrich B, Lenz O, Spahn CMT (2011b) The crystal structure of an oxygen tolerant hydrogenase uncovers a novel iron-sulphur centre. Nature 479:249–252

Garcin E, Vernede X, Hatchikian EC, Volbeda A, Frey M, Fontecilla-Camps JC (1999) The crystal structure of a reduced [NiFeSe] hydrogenase provides an image of the activated catalytic center. Structure 7:557–566

Gasper R, Scrima A, Wittinghofer A (2006) Structural insights into HypB, a GTP-binding protein that regulated metal binding. J Biol Chem 281:27492–27502

Goris T, Wait AF, Saggu M, Fritsch J, Heidary N, Stein M, Zebger I, Lendzian F, Armstrong FA, Friedrich B, Lenz O (2011) A unique iron-sulfur cluster is crucial for oxygen tolerance of a [NiFe]-hydrogenase. Nat Chem Biol 7:310–318

Hedderich R (2004) Energy-converting [NiFe] hydrogenases from archaea and extremophiles: ancestors of complex I. J Bioenerg Biomembr 36:65–75

Heering HA, Bulsink YBM, Hagen WR, Meyer TE (1995) Reversible super reduction of the cubane [4Fe-4S]$^{(3+,2+,1+)}$ in the high-potential iron-sulfur protein under nondenaturating conditions. Eur J Biochem 232:811–817

Helm ML, Stewart MP, Bullock RM, Rakowski DuBois M, DuBois DL (2011) A synthetic nickel electrocatalyst with a turnover frequency above 100,000 s^{-1} for H_2 production. Science 333:863–866

Higuchi Y, Ogata H, Miki K, Yasuoka N, Yagi T (1999) Removal of the bridging ligand atom at the Ni-Fe active site of [NiFe] hydrogenase upon reduction with H_2, as revealed by X-ray structure analysis at 1.4 Å resolution. Structure 7:549–556

Horch M, Lauterbach L, Lenz O, Hildebrandt P, Zebger I (2012) NAD(H)-coupled hydrogen cycling – structure-function relationships of bidirectional [NiFe] hydrogenases. FEBS Lett 586:545–556

Jones AK, Sillery E, Albracht SPJ, Armstrong FA (2002) Direct comparison of the electrocatalytic oxidation of hydrogen by an enzyme and a platinum catalyst. Chem Commun 8:866–867

Kaluarachchi H, Altenstein M, Sugumar SR, Balbach J, Zamble DB, Haupt C (2012) Nickel binding and [NiFe]-hydrogenase maturation by the metallchaperone SlyD with a single metal-binding site in *Escherichia coli*. J Mol Biol 417:28–35

Kröger A, Biel S, Simon J, Gross R, Unden G, Lancaster CRD (2002) Fumarate respiration of *Wolinella succinogenes*: enzymology, energetics and coupling mechanism. Biochim Biophys Acta 1553:23–38

Kumarevel T, Tanaka T, Bessho Y, Shinkai A, Yokoyama S (2009) Crystal structure of hydrogenase maturating endopeptidase HycI from *Escherichia coli*. Biochem Biophys Res Commun 389:310–314

Laurinavichene TV, Zorin NA, Tsygankov AA (2002) Effect of redox potential on activity of hydrogenase 1 and hydrogenase 2 in *Escherichia coli*. Arch Microbiol 178:437–442

Leonhartsberger S, Korsa I, Böck A (2002) The molecular biology of formate metabolism in enterobacteria. J Mol Microbiol Biotechnol 4:269–276

Loew C, Neumann P, Tidow H, Weininger U, Haupt C, Friedrich-Epler B, Scholz C, Stubbs MT, Balbach J (2010) Crystal structure determination and functional characterization of the metallochaperone SlyD from *Thermus thermophilus*. J Mol Biol 398:375–390

Lubitz W, Reijerse E, Van Gastel M (2007) [NiFe] and [FeFe] hydrogenases studied by advanced magnetic resonance techniques. Chem Rev 107:4331–4365

Lubner CE, Knörzer P, Silva PJ, Vincent KA, Happe T, Bryant DA, Golbeck JH (2010) Wiring an [FeFe]-hydrogenase with photosystem I for light-induced hydrogen production. Biochemistry 49:10264–10266

Lukey MJ, Parkin A, Roessler MM, Murphy BJ, Harmer J, Palmer T, Sargent F, Armstrong FA (2010) How *Escherichia coli* is equipped to oxidize hydrogen under different redox conditions. J Biol Chem 285:3928–3938

Lukey MJ, Roessler MM, Parkin A, Evans RM, Davies RA, Lenz O, Friedrich B, Sargent F, Armstrong FA (2011) Oxygen-tolerant [NiFe]-hydrogenases: the individual and collective importance of supernumerary cysteines at the proximal Fe-S cluster. J Am Chem Soc 133:16881–16892

Marques MC, Coelho R, De Lacey AL, Pereira IAC, Matias PM (2010) The three-dimensional structure of [NiFeSe] hydrogenase from *Desulfovibrio vulgaris* Hildenborough: a hydrogenase without a bridging ligand in the active site in its oxidised, "as-isolated" state. J Mol Biol 396:893–907

Matias PM, Soares CM, Saraiva LM, Coelho R, Morais J, Le Gall J, Carrondo MA (2001) [NiFe] hydrogenase from *Desulfovibrio desulfuricans* ATCC 27774: gene sequencing, three-dimensional structure determination and refinement at 1.8 Å and modelling studies of its interaction with the tetrahaem cytochrome c_3. J Biol Inorg Chem 6:63–81

Matias PM, Pereira IAC, Soares CM, Carrondo MA (2005) Sulphate respiration from hydrogen in *Desulfovibrio bacteria*: a structural biology overview. Prog Biophys Mol Biol 89:292–329

Montet Y, Amara P, Volbeda A, Vernede X, Hatchikian EC, Field MJ, Frey M, Fontecilla-Camps JC (1997) Gas access to the active site of Ni-Fe hydrogenases probed by X-ray crystallography and molecular dynamics. Nat Struct Biol 4:523–526

Nicolet Y, Piras C, Legrand P, Hatchikian CE, Fontecilla-Camps JC (1999) *Desulfovibrio desulfuricans* iron hydrogenase: the structure shows unusual coordination to an active site Fe binuclear center. Structure 7:13–23

Nicolet Y, De Lacey AL, Vernède X, Fernandez VM, Hatchikian EC, Fontecilla-Camps JC (2001) Crystallographic and FTIR spectroscopic evidence of changes in Fe coordination upon reduction of the active site of the Fe-only hydrogenase from *Desulfovibrio desulfuricans*. J Am Chem Soc 123:1596–1601

O'Hagan M, Shaw WJ, Raugei S, Chen S, Yang JY, Kilgore UJ, DuBois DL, Bullock RM (2011) Moving protons with pendant amines: proton mobility in a nickel catalyst for oxidation of hydrogen. J Am Chem Soc 133:14301–14312

Ogata H, Hirota S, Nakahara A, Komori H, Shibata N, Kato T, Kano K, Higuchi Y (2005) Activation process of [NiFe] hydrogenase elucidated by high-resolution X-Ray analyses: conversion of the ready to the unready state. Structure 13:1635–1642

Ogata H, Kellers P, Lubitz W (2010) The crystal structure of the [NiFe] hydrogenase from the photosynthetic bacterium *Allochromatium vinosum*: characterization of the oxidized enzyme Ni-a state. J Mol Biol 420:428–444

Page CC, Moser CC, Dutton ET (2003) Mechanism for electron transfer within and between proteins. Curr Opin Chem Biol 7:551–556

Pandelia ME, Ogata H, Lubitz W (2010) Intermediates in the catalytic cycle of [NiFe] hydrogenase: functional spectroscopy of the active site. ChemPhysChem 11:1127–1140

Pandelia ME, Nitschke W, Infossi P, Giudici-Orticoni MT, Bill E, Lubitz W (2011) Characterization of a unique [FeS] cluster in the electron transfer chain of the oxygen tolerant [NiFe] hydrogenase from *Aquifex aeolicus*. Proc Natl Acad Sci U S A 108:6097–6102

Pandelia ME, Lubitz W, Nitschke W (2012) Evolution and diversification of group 1 [NiFe] hydrogenases. Is there a phylogenetic marker for O_2-tolerance? Biochim Biophys Acta 1817:1565–1575

Parkin A, Goldet G, Cavazza C, Fontecilla-Camps JC, Armstrong FA (2008) The difference a Se makes? Oxygen-tolerant hydrogen production by the [NiFeSe]-hydrogenase from *Desulfomicrobium baculatum*. J Am Chem Soc 130:13410–13416

Parkin A, Bowman L, Roessler MM, Davies RA, Palmer T, Armstrong FA, Sargent FA (2012) How salmonella oxidises H_2 under aerobic conditions. FEBS Lett 586:536–544

Petkun S, Shi R, Li Y, Asinas A, Munger C, Zhang L, Waclawek M, Soboh B, Sawers RG, Cygler M (2011) Structure of hydrogenase maturation protein HypF with reaction intermediates shows two active sites. Structure 19:1773–1783

Pinske C, Krüger S, Soboh B, Ihling C, Kuhns M, Braussemann M, Jaroschinsky M, Sauer C, Sargent F, Sinz A, Sawers RG (2011) Efficient electron transfer from hydrogen to benzyl viologen by the [NiFe]-hydrogenases of *Escherichia coli* is dependent on the coexpression of the iron-sulfur-containing small subunit. Arch Microbiol 193:893–903

Pinske C, Jaroschinsky M, Sargent F, Sawers G (2012) Zymographic differentiation of NiFe]-hydrogenases 1, 2 and 3 of *Escherichia coli* K-12. BMC Microbiol 12:134. doi:10.1186/1471-2180-12-134

Poole RK, Hill S (1997) Respiratory protection of nitrogenase activity in *Azotobacter vinelandii*–roles of the terminal oxidases. Biosci Rep 17:303–317

Poole LB, Nelson KJ (2008) Discovering mechanisms of signaling-mediated cysteine oxidation. Curr Opin Chem Biol 12:18–24

Rangarajan ES, Asinas A, Proteau A, Munger C, Baardsnes J, Iannuzzi P, Matte A, Cygler M (2008) Structure of [NiFe] hydrogenase maturation protein HypE from *Escherichia coli* and its interaction with HypF. J Bacteriol 190:1447–1458

Redwood MD, Mikheenko IP, Sargent F, Macaskie L (2007) Dissecting the roles of *Escherichia coli* hydrogenases in biohydrogen production. FEMS Microbiol Lett 278:48–55

Reisner E, Armstrong FA (2011) A TiO_2 nanoparticle system for sacrificial solar H_2 production prepared by rational combination of hydrogenase with a ruthenium photosensitizer. Methods Mol Biol 743:107–117

Reisner E, Powell DJ, Cavazza C, Fontecilla-Camps JC, Armstrong FA (2009) Visible light-driven H_2 production by hydrogenases attached to dye-sensitized TiO_2 nanoparticles. J Am Chem Soc 131:18457–18466

Roessler MM, Evans RM, Davies RA, Harmer JR, Armstrong FA (2012) EPR spectroscopic studies of the Fe-S clusters in the O_2-tolerant [NiFe]hydrogenase Hyd-1 from *E. coli*, and characterization of the unique [4Fe-3S] cluster by HYSCORE. J Am Chem Soc 134:15581–15594

Shomura Y, Higuchi Y (2012) Structural basis for the reaction mechanism of S-carbamoylation of HypE by HypF in the maturation of [NiFe]-hydrogenases. J Biol Chem 287:28409–28419

Shomura Y, Komori H, Miyabe N, Tomiyama M, Shibata N, Higuchi Y (2007) Crystal structures of hydrogenase maturation protein HypE in the apo and ATP-bound forms. J Mol Biol 372: 1045–1054

Shomura Y, Yoon KS, Nishihara H, Higuchi Y (2011) Structural basis for [4Fe-3S] cluster in the oxygen-tolerant membrane-bound [NiFe]-hydrogenase. Nature 479:253–256

Soboh B, Kuhns M, Braussemann M, Waclawek M, Muhr E, Pierik AJ, Sawers RG (2012) Evidence for an oxygen-sensitive iron-sulfur cluster in an immature large subunit species of *Escherichia coli* [NiFe]-hydrogenase 2. Biochem Biophys Res Commun 424:158–163

Söderhjelm P, Ryde U (2006) Combined computational and crystallographic study of the oxidised states of [NiFe] hydrogenase. J Mol Struct (THEOCHEM) 770:199–219

Thauer RK, Kaster AK, Goenrich M, Schick M, Hiromoto T, Shima S (2010) Hydrogenases from methanogenic archaea, nickel, a novel cofactor and H_2 storage. Annu Rev Biochem 79:507–536

Thoden JB, Holden HM, Wesenberg G, Raushel FM, Rayment I (1997) Structure of carbamoyl phosphate synthetase: a journey of 96 Å from substrate to product. Biochemistry 36:6305–6316

Tremblay PL, Lovley DR (2012) Role of the NiFe hydrogenase Hya in oxidative stress defense in *Geobacter sulfurreducens*. J Bacteriol 194:2248–2253

Vignais MV, Billoud B (2007) Occurrence, classification and biological function of hydrogenases: an overview. Chem Rev 107:4206–4272

Vincent KA, Cracknell JA, Lenz O, Zebger I, Friedrich B, Armstrong FA (2005a) Electrocatalytic hydrogen oxidation by an enzyme at high carbon monoxide or oxygen levels. Proc Natl Acad Sci U S A 102:16951–16954

Vincent KA, Parkin A, Lenz O, Albracht SP, Fontecilla-Camps JC, Cammack R, Friedrich B, Armstrong FA (2005b) Electrochemical definitions of O_2 sensitivity and oxidative inactivation in hydrogenases. J Am Chem Soc 127:18179–18189

Vincent KA, Cracknell JA, Clark JR, Ludwig M, Lenz O, Friedrich B, Armstrong FA (2006) Electricity from low-level H_2 in still air – an ultimate test for an oxygen tolerant hydrogenase. Chem Commun 48:5033–5035

Vincent KA, Parkin A, Armstrong FA (2007) Investigating and exploiting the electrocatalytic properties of hydrogenases. Chem Rev 107:4366–4413

Volbeda A, Charon MH, Piras C, Hatchikian EC, Frey M, Fontecilla-Camps JC (1995) Crystal structure of the nickel-iron hydrogenase from *Desulfovibrio gigas*. Nature 373:580–587

Volbeda A, Montet Y, Vernède X, Hatchikian EC, Fontecilla-Camps JC (2002) High resolution crystallographic analysis of *Desulfovibrio fructosovorans* [NiFe] hydrogenase. Int J Hydrog Energy 27:1449–1461

Volbeda A, Martin L, Cavazza C, Matho M, Faber BW, Roseboom W, Albracht SPJ, Garcin E, Rousset M, Fontecilla-Camps JC (2005) Structural differences between the ready and unready oxidized states of [NiFe]-hydrogenases. J Biol Inorg Chem 10:239–249

Volbeda A, Amara P, Darnault C, Mouesca J-M, Parkin A, Roessler MM, Armstrong FA, Fontecilla-Camps JC (2012) X-ray crystallographic and computational studies of the O_2-tolerant [NiFe]-hydrogenase 1 from *Escherichia coli*. Proc Natl Acad Sci U S A 109:5305–5310

Watanabe S, Matsumi R, Arai T, Atomi H, Imanaka T, Miki K (2007) Crystal structures of HypC, HypD and HypE: insights into cyanation reaction by thiol redox signaling. Mol Cell 27:29–40

Watanabe S, Arai T, Matsumi R, Atomi H, Imanaka T, Miki K (2009) Crystal structure of HypA, a nickel-binding metallochaperone for [NiFe] hydrogenase maturation. J Mol Biol 394:448–459

Xia W, Li H, Sze K-H, Sun H (2009) Structure of a nickel chaperone, HypA, from *Helicobacter pylori* reveals two distinct metal binding sites. J Am Chem Soc 131:10031–10040

http://www.springer.com/978-94-017-8553-2

Microbial BioEnergy: Hydrogen Production
Zannoni, D.; De Philippis, R. (Eds.)
2014, XXXV, 366 p. 66 illus., 55 illus. in color.,
Hardcover
ISBN: 978-94-017-8553-2